

Effect of vitamin B17 (amygdalin) found in apricot kernel on the irradiated salivary glands of albino rats

Dalia Mostafa Abdaulmoneam^{B–D}, Maha Hassan Bashir^{A,E,F}, Dalia Abdel Hamed El Baz^{A,E,F}

Department of Oral Biology, Faculty of Oral and Dental Medicine, Cairo University, Egypt

A – research concept and design; B – collection and/or assembly of data; C – data analysis and interpretation;
D – writing the article; E – critical revision of the article; F – final approval of the article

Dental and Medical Problems, ISSN 1644-387X (print), ISSN 2300-9020 (online)

Dent Med Probl. 2023;60(3):473–481

Address for correspondence

Dalia Mostafa Abdaulmoneam
E-mail: dr.daliaelfishawy@gmail.com

Funding sources

None declared

Conflict of interest

None declared

Acknowledgements

None declared

Received on September 19, 2020

Reviewed on December 27, 2020

Accepted on January 13, 2021

Published online on September 30, 2023

Abstract

Background. Radiotherapy is used as a treatment for head and neck cancers but increases the risk of salivary gland hypofunction. The management strategies include pharmacotherapies such as salivary substitutes and sialagogues which are largely temporary. In this study, we examine the regenerative potential of vitamin B17 to improve salivary gland function.

Objectives. The present investigation aims to identify the effect of vitamin B17 (amygdaline) on the irradiated parotid salivary gland of albino rats.

Material and methods. Twenty-eight adult male albino rats were randomly divided into two groups subjected to irradiation procedure. Fourteen were in the control group, receiving a daily 5 mL saline by oral gavage (7 rats for 14 days and 7 rats for 30 days) while the other fourteen were treated with a daily dose of vitamin B17 (grounded apricot kernel; GAK) at 400 mg/kg in 5 mL of saline by oral gavage (7 rats for 14 days and 7 rats for 30 days). The parotid glands were dissected from the two groups at 14 and 30 days from the day of exposure to irradiation. The parotid gland sections were subjected to H&E stain, immunohistochemical localization of epidermal growth factor (EGF) and PCR using transforming growth factor beta 2 (TGF- β 2).

Results. The histological abnormalities corroborate with the immunohistochemical localization of EGF and the PCR results of TGF β 2, as their up-regulation in the control group demonstrate oxidative stresses and inflammation. The Treatment with GAK decreased oxidative stress and inflammation while promoting tissue regeneration.

Conclusions. Vitamin B17 is a promising anti-inflammatory agent that boosts immunity, as the experimental group showed better histological architecture of the parotid gland than the other one.

Keywords: irradiation, parotid gland, vitamin B17, amygdalin, ground apricot kernel

Cite as

Abdaulmoneam DM, Bashir MH, El Baz DAH. Effect of vitamin B17 (amygdalin) found in apricot kernel on the irradiated salivary glands of albino rats. *Dent Med Probl.* 2023;60(3):473–481. doi:10.17219/dmp/132387

DOI

10.17219/dmp/132387

Copyright

Copyright by Author(s)

This is an article distributed under the terms of the Creative Commons Attribution 3.0 Unported License (CC BY 3.0) (<https://creativecommons.org/licenses/by/3.0/>).

Introduction

Radiation therapy is a double-edged sword, commonly used to treat patients with head and neck squamous cell carcinoma with negative consequences for salivary glands hypo-function.¹ Forty percent of patients exposed to radiotherapy, suffered from induced impairment of salivary gland function and consequent xerostomia (dry mouth), leading to a detrimental impact on oral health and quality of life.² Ionizing radiation has direct and indirect effects on macromolecules. Living cells absorb ionizing radiation directly disrupting atomic structures, leading to chemical and biological changes. It causes radiolysis of cellular water, generating reactive chemical species by activating oxidases and nitric oxide synthases. It disturbs mitochondrial functions significantly contributing to persistent alterations in lipids, proteins, nuclear DNA (nDNA) and mitochondrial DNA (mtDNA). Eventually, results in physical and chemical damage to tissues that may lead to cell death or neoplastic transformation. In many cases, ionizing radiation-induced cell death has been identified as apoptosis.³

Exposure of salivary glands to radiotherapy leads to a significant loss of acinar cells. However, the mechanism of this cellular attrition is widely debatable. Fibrosis and loss of tissue occur after the loss of function, and the onset and severity of this phase of cellular damage differ among the various species. Even if the fibrosis is not extensive, Loss of salivary fluid secretion still leads to xerostomia and associated complications such as difficulty swallowing, rampant dental caries, oral mucosal lesions and fungal infection.⁴

Thus, the mechanism involved in the irradiation-induced loss of salivary gland function is a subject of great interest in the field, with clinical studies directed towards assessing therapies targeted to the recovery of cell function, prevention of functional loss, or regeneration of salivary glands.⁵

The management strategies include stringent dental and oral hygiene and pharmacotherapies, such as salivary substitutes and sialagogues. Mandelonitrile beta-D-gentiobioside, which is commonly known as vitamin B17, is a natural cyanide-containing substance called nitriloside. Laetrile or amygdaline, the extract form of vitamin B17, is effective in treating cancer as it targets and destroys mutated cells, acts as an anti-inflammatory agent and boosts immunity.⁶

It is mandatory to provide clinically safe and efficient radioprotection agents to scavenge reactive oxygen species (ROS) and reduce the risks of radiotherapy. Antioxidants (AOs) are the primary key of protection against the damage of free radical ions and are essential for maintaining optimum health. Antioxidants have shown potential benefits in preventing or counteracting cellular damage, cancer, ageing, and other diseases.⁷

Epidermal growth factor (EGF) is a transmembrane protein that stimulates cell growth by binding to epidermal growth factor receptor (EGFR) with intrinsic tyrosine kinase activity, to excite target cells. The receptor undergoes dimerization and auto-phosphorylation upon the interaction with EGF-EGFR. It has another role in regulating the expression level of various transcription factors through multiple signaling pathways.⁸

Transforming growth factor beta 2 (TGF- β 2) is a multifunctional protein playing an important role in the process of development throughout life, controlling various cellular activities.⁹ It is also important in the process of angiogenesis, cell growth, apoptosis, cell migration, cell differentiation, cell-matrix remodeling, epithelial-mesenchymal transition, and wound healing.¹⁰

Since all the previously mentioned methods are only transient as they do not treat causes of xerostomia, they do not treat the salivary gland dysfunction but only provide symptomatic relief for dry mouth. Therefore, there is an unmet need for new treatment strategies for long-term salivary gland regeneration with minimal adverse effects and greater potency.¹¹

Material and methods

The experiment was conducted according to the guidelines of the Care and Use of Laboratory Animals 8th Edition 2011, in the animal facility within the Faculty of Medicine, Cairo University (Approval No: CU/III/S/93/17).

Preparation of the material

Vitamin B17 (amygdaline) was obtained by grinding apricot kernels and administered via gavage to the rats. Amygdaline was given in a dose of 400 mg/kg ground apricot kernel (GAK).¹²

Apricots (*Prunus armeniaca* L.) were purchased from the local fruit market. Apricot seeds contain approximately 20–80 μ mol/g of amygdalin.¹³ Apricot flesh was removed from fruits; the apricot outer shell was washed with tap water and air-dried at 30°C for about 2 weeks, then the outer shell of the apricot was cracked manually and the edible part (kernel) was stored at -20°C in sealed plastic bags until used. The apricot kernels were soaked in warm distilled water for 1 h to facilitate the manual removal of the thin layer coat on the kernel. Apricot kernels were ground and dissolved in saline to be given intragastrically to the rats. The GAK was prepared freshly within 1 h before administration.

Experimental animals

Rattus Norvegicus were used in this study since they are genetically similar. Notably, the albino with its red eyes and white fur is an iconic model organism for scientific research in a variety of fields.¹⁴

Twenty-eight 3-4 month old adult male albino rats weighing approximately 200 g were obtained from the animal facility, Faculty of Medicine, Cairo University. All the rats were subjected to a single dose of gamma-radiation of 5 Gy at the National Center for Radiation Research and Technology (NCRRT), housed by the Atomic Energy Authority, Cairo, Egypt. Irradiation was performed by using Canadian Gamma Cell-40 biological irradiator ($^{137}\text{-cesium}$), manufactured by the Atomic Energy of Canada Limited, Ontario, Canada.

Housing

The rats were allowed to acclimatize for one week before the experiment. They were housed in individual cages and maintained at a temperature of 20-24 C in a 12:12 h light: dark cycle during the experiments and fed with standard food pellets and tap water ad libitum.

Allocation and blinding

The rats were randomly grouped by an online random number generator (random.org). All the histological sections and the histomorphometric analysis were scored by two independent observers blind to the rats' group identities. The scores given by the observers for each section were averaged and used in further analysis.

Study design

The animals were divided into two groups of 14: group A received 5 ml of intragastric saline (no treatment just placebo) daily, immediately after irradiation; and group B received a single intragastric dose of 400 mg/kg (GAK containing vitamin B17) immediately after irradiation.

Half of the rats in each group (7 rats) were sacrificed on day 14 and the other half were sacrificed on day 30. The parotid glands were dissected out, fixed in calcium formalin and embedded in paraffin. Specimen were mounted on glass slides for H&E & immunohistochemical staining. Using an image analyzer, the optical density of immunohistochemical staining of EGF in terms of percent of the total area was calculated by digital image analysis.

Animals were anesthetized with ketamine HCL 50 mg/kg then trans-cardially perfused with 4% formaldehyde. The parotid salivary glands were dissected and collected for histological and histochemical examination.

The flow chart of the study design is presented in Fig. 1.

Methods of investigation

Histological evaluation

Hematoxylin & eosin stains are commonly employed for histologic and medical studies. Sections were deparaffinized and placed in xylene, hydrated by passing

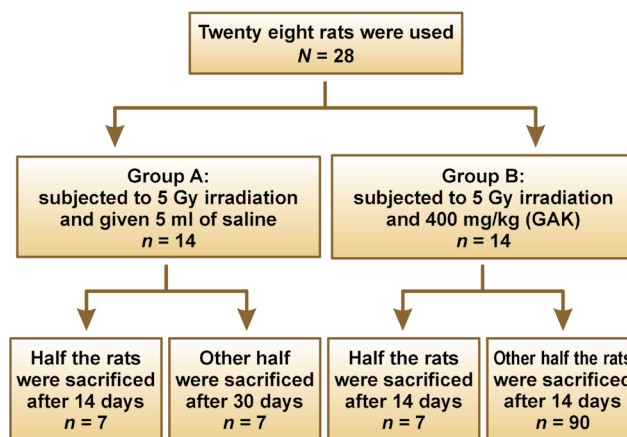


Fig. 1. Flowchart of the study design

through descending concentrations of alcohol baths and water. 95% alcohol for 2 minutes and 70% alcohol for 2 minutes followed by distilled water. The sections were then immersed in Harris hematoxylin solution for 8 minutes, differentiated in 1% acid alcohol for 30 seconds and washed in running tap water for 1 minute. Hematoxylin was "blued" in 0.2% ammonia water or saturated lithium carbonate solution for 30-60 seconds. Followed by another wash under running tap water for 5 minutes and a rinse in 95% alcohol. The sections were counterstained with eosin-phloxine solution for 30-60 seconds, dehydrated through 95% alcohol with 2 changes 5 min absolute alcohol washes. Finally, the sections were cleared in 2 changes 5 min of xylene washes and mounted with xylene based mounting medium. Sections were dehydrated in increasing concentrations of alcohols and cleared in xylene.¹⁵

Immunohistochemistry

It was used to measure the expression of EGF. Routine immunostaining procedures were applied to stain formalin-fixed and paraffin-embedded sections.

Five micron-thick sections were used. Specimens were dewaxed in 3 × 5 min xylol washes. The tissue specimen was placed into a glass slide chamber and filled with the processing buffer (citric acid buffer, pH 6.0, preferably pH 6.5-7.0) and incubated at 121°C for 15 min for antigen retrieval. The glass slides were taken out of the chamber, rinsed 3 times with distilled water or PBS by emptying and refilling the chambers 40 min after. Three to four drops of 1:50 primary monoclonal mouse anti-EGF antibodies in PBS were used on the sections for a 20 minute incubation. Endogenous peroxidase activity was blocked by using freshly made 0.3% H₂O₂ in methanol for 20 min followed by 3-5 min PBS washes. Incubation with monoclonal antibody, 4°C, overnight. On the next day, the sections were washed with PBS for three 5 min washes and incubated (60-120 min) with the secondary antibody, MAX-PO(MULTI) at room temperature. An-

other three 5 min washes with PBS was performed before applying the diaminobenzidin (filtered (0.01% DAB in 0.5 M Tris/HCl (pH 7.4)) substrate for 10 min at room temperature. H_2O_2 was added to a final concentration of 0.01%. At the end of the chromogenic staining, the sections were washed with running tap water for 3 min and counterstained with Mayer's hematoxylin for 30 s. After a brief rinse with tap water, the sections were dehydrated with increasing concentrations of ethanol: 50%, 70%, 96%, absolute for 3 min. each. Specimens were cleared with xylol with 3×3 min washes and mounted with mounting medium.¹⁶

Histomorphometric analysis of immunohistochemical staining

The immunostained sections were examined using an image analyzer computer system to measure the optical density in percent area. Immunoreactivity of EGF was performed through the images analysis using a computer (Leica Quin 500 Microsystems, Switzerland) consisting of color video camera connected to the microscope for image acquisition through a PC. The intensity of the reaction within the cells was determined by measuring the optical density in 5 small sampling fields in each section under 400x. The areas showing EGF positive brown immune staining were chosen for evaluation, regardless of the staining intensity. These areas were masked by a blue binary color to be measured by the computer system. The image analyzer is calibrated automatically to convert the measurement units produced by the image analyzer program into actual micrometer units. Mean values and standard deviations were calculated for each specimen.

Quantitative real-time PCR

It was used to measure the expression of TGF- β 2.

Total RNA was isolated using Qiagen tissue extraction kit (Qiagen, USA) according to the instructions of the manufacturer. The total RNA (0.5–2 μ g) was used for cDNA conversion using high capacity cDNA reverse transcription kit Fermentas, USA). Real-time qPCR amplification and analysis were performed using an Applied Biosystem software version 3.1 (StepOne™, USA). The qPCR assay with the primer sets was optimized at the annealing temperature. The relative quantitation was calculated according to Applied Biosystem software.

Statistical analysis

ANOVA was used to compare between all conditions. Data are presented as the mean \pm standard deviation (SD). A p-value of $p < 0.001$ was considered to be statistically significant. This was followed by Tukey's post hoc test when ANOVA indicated a significant difference.

Results

Histological examination

The H&E stained sections of group A (irradiated only) showed degenerative changes at both day 14 and day 30. Acinar shrinkage, multiple cytoplasmic vacuoles and nuclear anisonucleosis and poikilonucleosis were detected. The duct system showed thinning of the epithelial lining of some excretory ducts and stagnant secretion was found in others. Both intercalated and striated ducts showed no detectable changes. Areas of fibrosis were detected in the connective tissue that was chronically infiltrated by inflammatory cells. Additionally, the blood vessels suffered from dilatation and some appeared engorged with RBCs. Also, some blood vessels showed hyalinization and others were ruptured (Fig.2,3).

On the contrary, the H&E stained sections of group B (irradiated group receiving treatment) on day 14 showed improved degenerative changes that further improved at

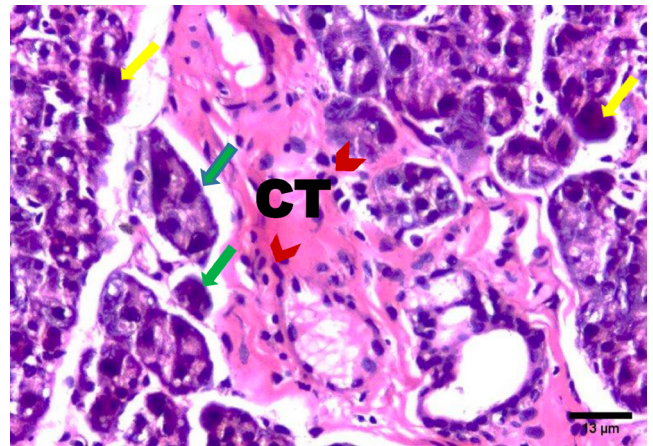


Fig. 2. Photomicrograph of rat parotid gland of group A (day 14) showing: shrunken acini (green arrows), acini showing clumping (yellow arrows), fibrosis in connective tissue (CT), inflammatory cells (red arrow heads), excretory duct showing signs of degeneration (red arrow) (H&E, Orig. Mag. x400)

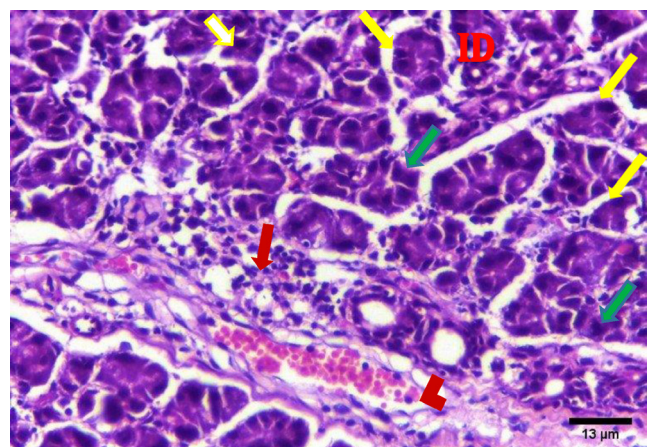


Fig. 3. Photomicrograph of rat parotid gland of group A (day 30) showing: shrunken acini (yellow arrows), clumped acini (white arrow), dilated blood vessels engorged with RBCs (red arrow head), nuclear anisonucleosis & poikilonucleosis (green arrows), inflammatory cells within connective tissue (red arrow), intercalated duct seems to be normal (ID) (H&E, Orig. Mag. x400)

day 30. The positive outcome is demonstrated by decreased acinar shrinkage and cytoplasmic vacuolization in some acini, others suffered from degeneration in a few areas, also nuclear anisonucleosis and poikilonucleosis were less pronounced in this group. Mitotic figures were observed within some acinar cells. The striated and intercalated ducts maintained their form and remained intact. Few excretory ducts showed areas of thinning in their epithelial lining. The connective tissue appeared with fewer areas of fibrosis and few chronic inflammatory cells infiltrated. Few blood vessels were dilated and engorged with RBCs (Fig. 4,5).

Immunohistochemical examination

Immunohistochemical investigation of parotid glands of group A on day 14 revealed strong cytoplasmic, membranous and nuclear expression of EGF in both acini and ducts. There was no staining in the connective tissue. Immunostained specimens from the same group on day 30

showed strong membranous, cytoplasmic and nuclear expression of the EGF in acinar & ductal cells. Few scattered serous cells showed no nuclear expression. The connective tissue showed no expression (Fig. 6,7).

Immunohistochemical investigation of parotid glands of group B on day 14 showed weak membranous, moderate cytoplasmic and nuclear reactivity of acinar cells. Some acinar cells showed no nuclear expression. The ductal cells showed strong membranous, cytoplasmic and nuclear expression. There was no immunoreactivity in the connective tissue. Immunostained sections from the same group on day 30 showed weak membranous, cytoplasmic and negative nuclear expression in serous cells. The duct system revealed strong membranous, cytoplasmic and nuclear expression. The connective tissue did not stain for EGF (Fig. 8,9).

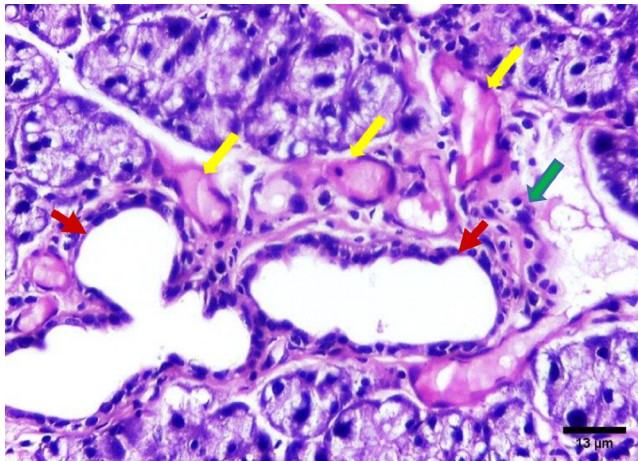


Fig. 4. Photomicrograph of a rat parotid gland of group B (day 14) showing: hyalinized blood vessels with discontinuity in their linings (yellow arrows), excretory duct showing thinning in their lining (red arrows), inflammatory cells infiltration (green arrow) (H&E, Orig. Mag. x400)

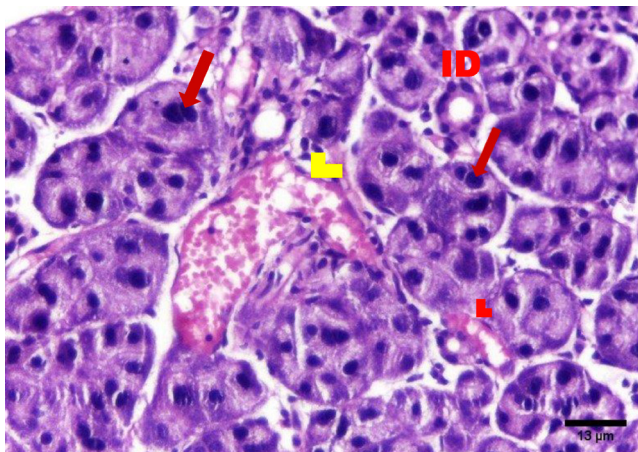


Fig. 5. Photomicrograph of a rat parotid gland of group B (day 30) showing: mitotic figures within acinar cells (red arrows), dilated blood vessels engorged with RBCs (yellow arrow head), hyalinized blood vessel (red arrow head), normally appearing intercalated ducts (ID) (H&E, Orig. Mag. x400)

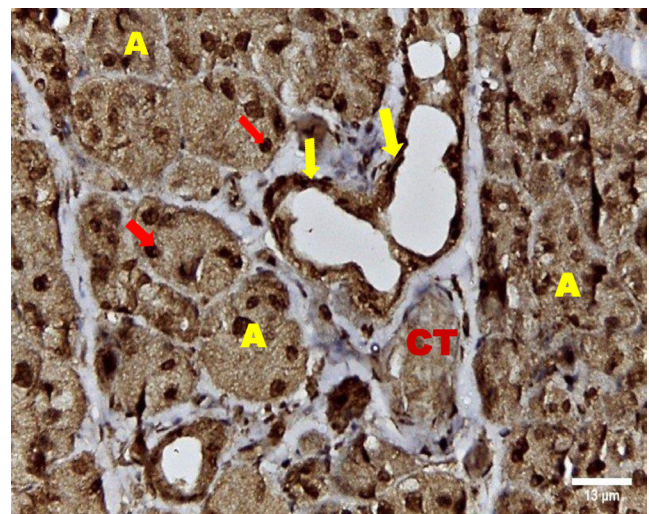


Fig. 6. Photomicrograph of a rat parotid gland of group A (day 14) showing immunoreactivity of EGF: strong membranous, cytoplasmic (A) and nuclear (red arrows) expression within serous acini, excretory duct showing strong membranous, cytoplasmic and nuclear expression (yellow arrows), and negative expression within the connective tissue (CT) (DAB, Orig. Mag. x400)

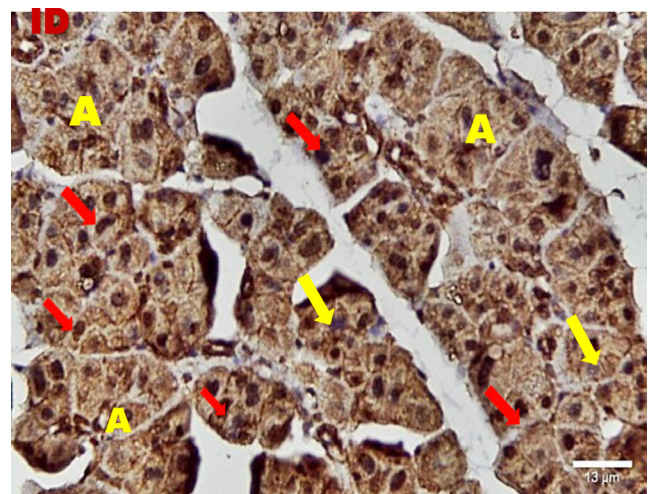


Fig. 7. Photomicrograph of a rat parotid gland of group A (day 30) showing immunoreactivity of EGF: strong membranous, cytoplasmic (A), and nuclear (red arrows), acinar cells with negative nuclear expression (yellow arrows), strong membranous, cytoplasmic & nuclear expression within intercalated duct (ID) (DAB, Orig. Mag. x400)

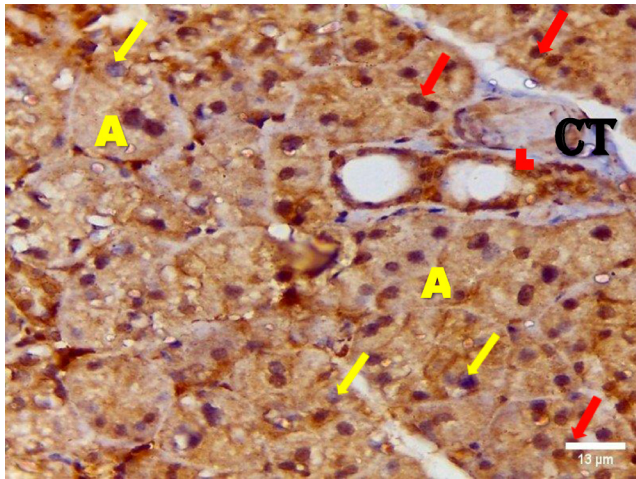


Fig. 8. Photomicrograph of a rat parotid gland of group B (day 14) showing immunoreactivity of EGF: weak membranous, moderate cytoplasmic (A), moderate nuclear (red arrows), negative nuclear (yellow arrows), expression within serous acini, excretory duct (red arrow head) showing strong membranous, cytoplasmic and nuclear expression, while connective tissue shows negative expression (CT) (DAB, Orig. Mag. x400)

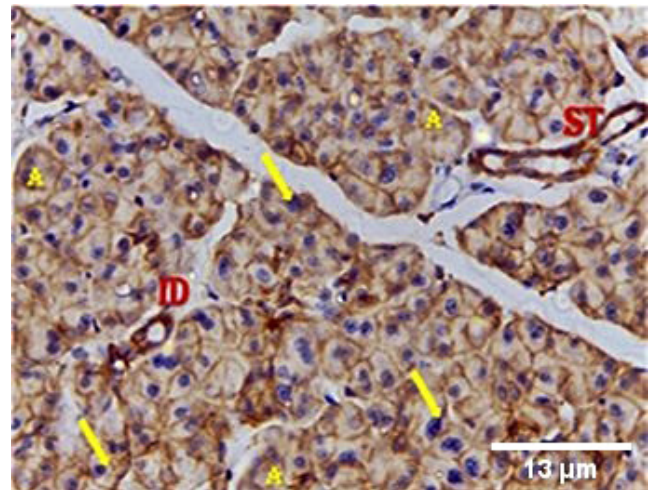


Fig. 9. Photomicrograph of a rat parotid gland of group B (day 30) showing immunoreactivity of EGF: weak membranous and cytoplasmic (A), negative nuclear expression (yellow arrows) within serous acini, intercalated duct (ID) and striated duct (ST) showing strong membranous, cytoplasmic and nuclear expression (DAB, Orig. Mag. x400)

Statistical analysis

Immunohistochemical analysis was quantified using percent area. The analysis suggests the mean EGF expression covered more tissue area in group A compared to group B. ANOVA test revealed that the difference was statistically significant ($P < 0.0001$) between all the studied groups. Tukey's post hoc test revealed no significant difference between group B at 14 days and group A at 30 days. Moreover, no significant difference could be observed between group B at 14 and 30 days (Table 1, Fig. 10).

PCR results of TGF- β 2 revealed that the greatest mean value was detected in group A while the lowest mean value was recorded in group B. ANOVA test revealed that the difference was statistically significant ($P < 0.0001$) between all

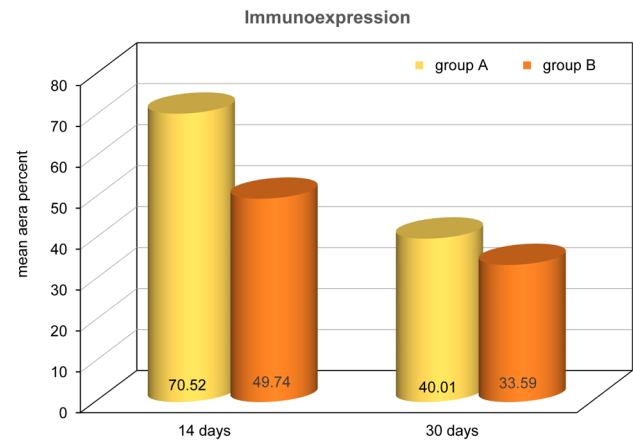


Fig. 10. Column chart showing mean area percent of EGF immunoreactivity in Group A and Group B at each date

Table 1. Area percentage of immunoreactivity of epidermal growth factor (EDF) in different groups (ANOVA)

Group	Time point	$M \pm SD$	SE	95% CI		min	max	F	p-value
				lower bound	upper bound				
Group A	day 14	70.52 \pm 12.73 ^a	5.69	54.71	86.33	58.43	89.78	18.25	<0.0001*
	day 30	49.74 \pm 5.03 ^b	2.25	43.49	55.99	43.42	57.50		
Group B	day 14	40.01 \pm 8.38 ^{b,c}	3.75	29.60	50.41	26.98	49.92		
	day 30	33.59 \pm 5.26 ^c	2.35	27.05	40.12	25.35	39.12		

* statistically significant; values with different superscript letters are significantly different (Tukey's post hoc test).

Table 2. Mean values of transforming growth factor beta 2 (TGF- β 2) in different groups (ANOVA)

Group	Time point	$M \pm SD$	SE	95% CI		min	max	F	p-value
				lower bound	upper bound				
Group A	day 14	2.92 \pm 0.13 ^a	0.06	2.76	3.08	2.73	3.06	188.49	<0.0001*
	day 30	2.37 \pm 0.26 ^b	0.11	2.05	2.69	2.10	2.66		
Group B	day 14	1.23 \pm 0.05 ^c	0.02	1.17	1.30	1.15	1.30		
	day 30	0.87 \pm 0.11 ^d	0.05	0.74	1.00	0.74	0.99		

* statistically significant; values with different superscript letters are significantly different (Tukey's post hoc test).

studied groups. This was followed by Tukey's post hoc test when ANOVA indicated a significant difference. Tukey's post hoc test revealed a statistically significant difference between the two subgroups (Table 2, Fig. 11).

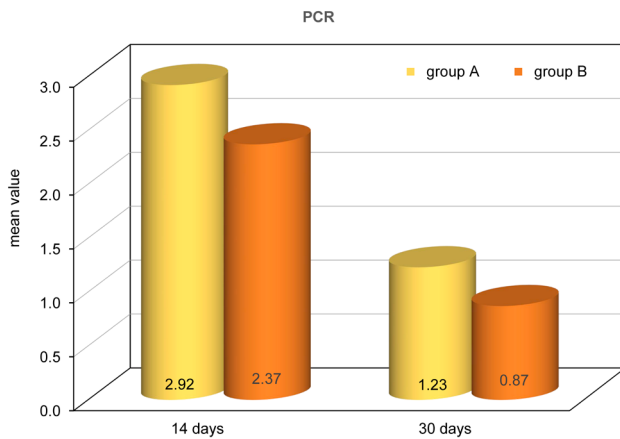


Fig. 11. Column chart showing mean values of TGF- β 2 in group A and group B at each date

Discussion

Acinar cells in the salivary gland are destroyed during radiation treatment for head and neck cancer that results in a lifetime of hyposalivation and co-morbidities.¹⁷ In the present investigation, a sub-lethal dose of radiation at 5 Gy was used.¹⁸ The chosen radiation dose was selected similar to Avila who used the same ionizing radiation dose and reported radiation-induced changes in the parotid gland of rats.⁵

The results of the present study showed acinar degeneration, shrinkage and cytoplasmic vacuolization in group A (day 14 and day 30). Boraks, Tampelini, Pereira, and Chopard have linked acinar degeneration and vacuolization to the expansion of the endoplasmic reticulum which is associated with the cellular status that precedes apoptosis this expansion is related to compression of the nuclear material.¹⁹

In the current investigation, shrinkage of some serous acini, fewer areas of acinar degeneration and fewer cytoplasmic vacuoles were observed within some serous acini in group B which received vitamin B17 (day 14 and day 30). The changes on day 30 were less than that on day 14. These changes were similar to findings reported by Qadir and Fatima where amygdalin acts as an antioxidant and a scavenger of the harmful and highly hydroxyl radicals by maintaining a healthy body pH.²⁰

Moreover, the observed nuclear changes (anisonucleosis & poikilonucleosis) and clumped acini with condensed chromatin reported in this work are in agreement with Krishnan et al. who observed shrunken nuclei with condensed chromatin in irradiated salivary gland acinar cells.

The author assumed that the irradiation dose was not high enough to cause complete DNA destruction and complete nuclear disintegration.²¹

Intercalated and striated ducts showed no detectable changes in our study in group A (day 14 and day 30) and group B (day 14 and day 30). This could be attributed to the powerful regenerative properties of the ductal structure of the salivary gland.²²

In the present investigation, excretory ducts showed degeneration of their lining, others showed stagnant secretion in group A (after 14 days). These findings corroborate with those reported by Kassab, and Tawfik who detected degeneration of excretory duct and stagnant secretion due to oxidative stresses and inflammation in albino rats subjected to long term use of caffeinated drinks.²³

In this study, the stagnant secretion found in some excretory ducts in group A was previously shown by Halawa, Mohamed, and Obeid who found some dilated excretory duct with stagnant secretion and concluded that the mitochondrion is the most vulnerable cell organelle to toxic agents and oxidative stresses. Upon mitochondrial destruction in excretory ducts, cellular metabolism was affected with advanced cellular destruction. Destroyed mitochondria result in adenosine triphosphate ATP consumption and subsequently, impaired exocytosis took place, so no energy for secretion causing stagnant secretion and ductal dilatation.²⁴

In the current work, connective tissue fibrosis was noted mainly in group A (day 14 and day 30), consistent with Huang, Chen, and Miao who demonstrated that the connective tissue stroma of parotid and submandibular gland of rats undergoes adiposis and fibrosis after irradiation.²⁵

Milazzo et al. reported that vitamin B17 which is a main component of GAK has many potentialities in addition to its protective effect against cancer. It boosts immunity and eliminates harmful cells as it acts as an antioxidant. The protective properties could account for the decreased fibrosis in group B (day 14 & day 30) in this study.⁶ This interpretation is supported by Abdel-Rahman who carried out a study on rats suffering from induced hepatic fibrosis and reported that the addition of GAK to rats' diet inhibited acute hepatocellular injury and fibrosis.¹²

The presence of blood vessels engorged with red blood cells was observed in this investigation in group A (14 and 30 days) which decreased in group B (14 & 30 days). These findings were in agreement with the results of Redman who found thinning and discontinuity in the endothelium lining of blood vessels of the parotid salivary gland of rats that was subjected to irradiation, leading to a compromised blood supply.²⁶

Chronic inflammatory cells infiltration in the connective tissue in this study were clearly observed in group A (day 14 & day 30), replicating findings by Limesand, Said, and Anderson, who found chronic inflammatory cells in response to irradiation of parotid salivary glands of rats.²⁷

Chronic inflammatory cells and dilated blood vessels decreased in the treatment group at 14 days with continued improvements at day 30 compared to controls. These observations may be mediated by the anti-inflammatory properties of GAK, where Minaiyan, Ghannadi, Asadi, Etemad, and Mahzouni found GAK treatment in treating colon inflammation in rats also resulted in a decrease in inflammatory cells.²⁸

Mitotic figures were observed in group B specifically on day 30. This finding was explained by Mohamed, El-Sakhawy, Sheriff, and Shredah, who assumed that mononuclear cells duplicate DNA while undergoing endomitosis. Therepeated prevalence of mitotic figures can be explained by being an adaptive trial of the acinar cells to heal after injury.²⁹

Noticeably, the immunohistochemical results in the current study supported the histological results - strong cytoplasmic, membranous and nuclear EGF expression of acini and ducts in group A on day 14 and day 30 was observed. These results were in agreement with Shang et al. who demonstrated upregulation of EGF in most mucopidermoid carcinomas, which surges to 80% in case of lymph node metastases.³⁰

The results of this study demonstrated strong nuclear expression within the acini of group A at day 14 and day 30, which was clarified by Dittmann et al. who concluded that upon cell irradiation EGF-EGFR complex are translocated to the cell nucleus, principally in regions with uncoiled chromatin (euchromatin) because these areas are easily accessible for DNA repair processes after exposure to irradiation.³¹

Moreover, Vuorinen, Rajala, Ihalainen, and Kallioniemi found that the complex is linked to co-transport of some associated proteins such as Ku70 and Ku80 as well as protein phosphatase 1 which is linked to the nucleus and is involved in the regulation of DNA-protein kinase. Nuclear import of the EGFR-linked complex is permitted by a karyopherin-dependent process which plays an important role in the process of regeneration.³²

Group B in the current study demonstrated weak membranous, moderate cytoplasmic and nuclear reactivity on day 14, while on day 30 it showed weak membranous, cytoplasmic and no nuclear expression of EGF. These results were explained by Dittmann et al. who reported that the use of radical scavengers eliminated radiation-induced EGF nuclear translocation.³¹ Moreover, the connective tissue of all groups showed no EGF expression, which is in agreement with Zhuang, and Liu who assumed that EGF and EGFR are located mainly in epithelial cells not in the connective tissue under normal or pathologic conditions.³³

PCR results of this study are consistent with the histological and immunohistochemical results as they revealed an increase in the amount of TGF- β 2 in group A on day 14 and day 30, while this amount decreased in group B on day 14 and day 30, respectively.

The increase in TGF- β 2 levels in group A have been reported by Barrientos, Stojadinovic, Golinko, Brem, and Tomic, who suggested the involvement of TGF- β 2 in granulation tissue formation, through stimulation of angiogenesis, fibroblast proliferation, myofibroblast differentiation, and matrix deposition.³⁴

To the best of our knowledge, little or sparse documents were available on how ground apricot kernel (vitamin B17) affected irradiated parotid salivary glands, neither its potential effect on TGF- β 2 levels nor EGF expression.

Conclusions

A single dose of whole-body 5 Gy irradiation-induced degenerative changes of the parotid glands of albino rats. Administration of vitamin B17 (GAK) intragastric to the irradiated rats improved the histological features of the irradiated salivary gland. The histological results and the observed immunohistochemical localization of EGF and PCR results of TGF β 2 support the translational therapeutic potential of GAK on salivary gland dysfunction associated with oral cancers by downregulating oxidative damage and inflammatory responses.

Ethics approval and consent to participate

The experiment was conducted according to the "Guide for the Care and Use of Laboratory Animals" 8th ed., 2011, in the animal facility within the Faculty of Medicine, Cairo University, Egypt (approval No. CU/III/S/93/17).

Data availability

The datasets generated and/or analyzed during the current study are available from the corresponding author on reasonable request.


Consent for publication

Not applicable.

ORCID iDs

Dalia Mostafa Abdaulmoneam  <https://orcid.org/0000-0003-4682-4171>

Maha Hassan Bashir  <https://orcid.org/0000-0002-7833-695X>

Dalia Abdel Hamed El Baz  <https://orcid.org/0000-0002-2799-2666>

References

1. St John MA, Abemayor E, Wong DT. Recent new approaches to the treatment of head and neck cancer. *Anticancer Drugs*. 2006;17(4):365–375. doi:10.1097/01.cad.0000198913.75571.13
2. Van Luijk P, Pringle S, Deasy JO, et al. Sparing the region of the salivary gland containing stem cells preserves saliva production after radiotherapy for head and neck cancer. *Sci Transl Med*. 2015;7(305):305ra147. doi:10.1126/scitranslmed.aac4441
3. Azzam El, Jay-Gerin JP, Pain D. Ionizing radiation-induced metabolic oxidative stress and prolonged cell injury. *Cancer Lett*. 2012;327(1–2):48–60. doi:10.1016/j.canlet.2011.12.012

4. Ambudkar IS. Calcium signaling in salivary gland physiology and dysfunction. *J Physiol*. 2016;594(11):2813–2824. doi:10.1113/JP271143
5. Avila JL, Grundmann O, Burd R, Limesand KH. Radiation-induced salivary gland dysfunction results from p53-dependent apoptosis. *Int J Radiat Oncol Biol Phys*. 2009;73(2):523–529. doi:10.1016/j.ijrobp.2008.09.036
6. Milazzo S, Lejeune S, Ernst E. Laetrile for cancer: A systematic review of the clinical evidence. *Support Care Cancer*. 2006;15(6):583–595. doi:10.1007/s00520-006-0168-9
7. Payen VL, Porporato PE, Danhier P, et al. (+)-Catechin in a 1:2 complex with lysine inhibits cancer cell migration and metastatic take in mice. *Front Pharmacol*. 2017;8:869. doi:10.3389/fphar.2017.00869
8. Lemmon MA, Schlessinger J. Cell signaling by receptor tyrosine kinases. *Cell*. 2010;141(7):1117–1134. doi:10.1016/j.cell.2010.06.011
9. Tang S, Ou J, Sun D, Zhang Y, Xu G, Zhang Y. A novel 62-bp indel mutation in the promoter region of transforming growth factor-beta 2 (*TGFB2*) gene is associated with body weight in chickens. *Anim Genet*. 2011;42(1):108–112. doi:10.1111/j.1365-2052.2010.02060.x
10. Ishtiaq Ahmed AS, Bose G, Huang L, Azhar M. Generation of mice carrying a knockout-first and conditional-ready allele of transforming growth factor beta2 gene. *Genesis*. 2014;52(9):817–826. doi:10.1002/dvg.22795
11. Pringle S, Van Os R, Coppes RP. Concise review: Adult salivary gland stem cells and a potential therapy for xerostomia. *Stem Cells*. 2013;31(4):613–619. doi:10.1002/stem.1327
12. Abdel-Rahman MK. Can apricot kernels fatty acids delay the atrophied hepatocytes from progression to fibrosis in dimethylnitrosamine (DMN)-induced liver injury in rats? *Lipids Health Dis*. 2011;10:114. doi:10.1186/1476-511X-10-114
13. Patrikios I, Stephanou A, Yiallouris A. *Tripterygium wilfordii* extract (triptolide) and amygdalin promotes cell death in cancer cells: True or a myth. *Am J Cancer Prev*. 2015;3(4):77–83. doi:10.12691/ajcp-3-4-3
14. Jacob HJ, Brown DM, Bunker RK, et al. A genetic linkage map of the laboratory rat, *Rattus norvegicus*. *Nat Genet*. 1995;9(1):63–69. doi:10.1038/ng0195-63
15. Bancroft JD, Layton C. Connective and mesenchymal tissues with their stains. In: Suvarna KS, Layton C, Bancroft JD. *Bancroft's Theory and Practice of Histological Techniques*. 8th ed. Amsterdam, the Netherlands: Elsevier; 2012:187–214.
16. Journé F, Wattiez R, Severyns C, et al. Transforming growth factor-alpha and epidermal growth factor in hamster tissues: Biochemical and immunohistochemical studies. *Comp Biochem Physiol C Pharmacol Toxicol Endocrinol*. 1995;112(2):187–200. doi:10.1016/0742-8413(95)02011-x
17. May AJ, Cruz-Pacheco N, Emmerson E, et al. Diverse progenitor cells preserve salivary gland ductal architecture after radiation-induced damage. *Development*. 2018;145(21):dev166363. doi:10.1242/dev.166363
18. Williams JP, Brown SL, Georges GE, et al. Animal models for medical countermeasures to radiation exposure. *Radiat Res*. 2010;173(4):557–578. doi:10.1667/RR1880.1
19. Boraks G, Tampelini FS, Pereira KF, Chopard RP. Effect of ionizing radiation on rat parotid gland. *Braz Dent J*. 2008;19(1):73–76. doi:10.1590/s0103-64402008000100013
20. Qadir M, Fatima K. Review on pharmacological activity of amygdalin. *Arch Can Res*. 2017;5(4):160. doi:10.21767/2254-6081.1000160
21. Krishnan M, Tennavan A, Saraswathy S, Sekhri T, Singh AK, Nair V. Acute radiation-induced changes in Sprague–Dawley rat submandibular glands: A histomorphometric analysis. *World J Oncol*. 2017;8(2):45–52. doi:10.14740/wjon1021w
22. May AJ, Cruz-Pacheco N, Emmerson E, et al. Diverse progenitor cells preserve salivary gland ductal architecture after radiation-induced damage. *Development*. 2018;145(21):dev166363. doi:10.1242/dev.166363
23. Kassab AA, Tawfik SM. Effect of a caffeinated energy drink and its withdrawal on the submandibular salivary gland of adult male albino rats: A histological and immunohistochemical study. *Egypt J Histol*. 2018;41(1):11–26. doi:10.21608/EJH.2018.7518
24. Halawa AM, Mohamed DG, Adeeb Obeid RF. Capsaicin induced histological and ultrastructural changes in the submandibular salivary gland of albino rats. *Futur Dent J*. 2016;2(1):22–27. doi:10.1016/j.fdj.2016.04.002
25. Huang Y, Chen N, Miao D. Radioprotective effects of pyrroloquinoline quinone on parotid glands in C57BL/6J mice. *Exp Ther Med*. 2016;12(6):3685–3693. doi:10.3892/etm.2016.3843
26. Redman RS. On approaches to the functional restoration of salivary glands damaged by radiation therapy for head and neck cancer, with a review of related aspects of salivary gland morphology and development. *Biotech Histochem*. 2008;83(3–4):103–130. doi:10.1080/10520290802374683
27. Limesand KH, Said S, Anderson SM. Suppression of radiation-induced salivary gland dysfunction by IGF-1. *PLoS One*. 2009;4(3):e4663. doi:10.1371/journal.pone.0004663
28. Minaiyan M, Ghannadi A, Asadi M, Etemad M, Mahzouni P. Anti-inflammatory effect of *Prunus armeniaca* L. (apricot) extracts ameliorates TNBS-induced ulcerative colitis in rats. *Res Pharm Sci*. 2014;9(4):225–231. PMID:25657793. PMCID:PMC4314870.
29. Mohamed SS, El-Sakhawy MA, Sherif H, Shredah M. Effect of aspartame on submandibular salivary glands of adult male albino rats. *Life Sci J*. 2015;12(3):44–50. http://www.lifesciencesite.com/ljsj/life120315/007_28164life120315_44_50.pdf.
30. Shang J, Shui Y, Sheng L, Wang K, Hu Q, Wei Q. Epidermal growth factor receptor and human epidermal growth receptor 2 expression in parotid mucoepidermoid carcinoma: Possible implications for targeted therapy. *Oncol Rep*. 2008;19(2):435–440. PMID:18202792.
31. Dittmann K, Mayer C, Fehrenbacher B, et al. Radiation-induced epidermal growth factor receptor nuclear import is linked to activation of DNA-dependent protein kinase. *J Biol Chem*. 2005;280(35):31182–31189. doi:10.1074/jbc.M506591200
32. Vuorinen EM, Rajala NK, Ihalainen TO, Kallioniemi A. Depletion of nuclear import protein karyopherin alpha 7 (KPNA7) induces mitotic defects and deformation of nuclei in cancer cells. *BMC Cancer*. 2018;18(1):325. doi:10.1186/s12885-018-4261-5
33. Zhuang S, Liu N. (2014). EGFR signaling in renal fibrosis. *Kidney Int Suppl (2011)*. 2014;4(1):70–74. doi:10.1038/kisup.2014.13
34. Barrientos S, Stojadinovic O, Golinko MS, Brem H, Tomic-Canic M. Growth factors and cytokines in wound healing. *Wound Repair Regen*. 2008;16(5):585–601. doi:10.1111/j.1524-475X.2008.00410.x